

FGM vs ATFM: a comparative analysis in predicting the flame characteristics of an industrial swirler

G. Lemmi*, **P.C. Nassini***, **S. Castellani***, **A. Picchi***, **S. Galeotti***, **R. Becchi***, **A. Andreini***, **G. Babazzi****, **R. Meloni****

gianmarco.lemmi@unifi.it

*Department of Industrial Engineering, University of Florence, Italy

**Baker Hughes, Via F. Matteucci 2, 50127, Florence, Italy

Abstract

The present work focuses on the comparison between two of the most used combustion models, the Flamelet Generated Manifold (FGM) and the Artificially Thickened Flame Model (ATFM), when applied to an industrial lean premixed burner operated with methane at atmospheric pressure. Both the models represent extended versions specifically intended to overcome their respective limitations. Detailed chemiluminescence images revealing the flame shape and position will represent the main benchmark for the numerical validation. Furthermore, the differences in terms of flow field and fuel concentration at the burner exit will be shown as well as the overall CO prediction.

Introduction

Reactive Computational Fluid Dynamics (CFD) codes rely on just few models whose performance can be design-dependent and/or extremely sensible to the fuel composition as well. Detailed experimental measurements of the flame are extremely useful for the validation of such models allowing the designers to know *when-and-how* a combustion model can be preferred to another one and at which computational cost. Nowadays the literature is dominated by two families of combustion models: the tabulated-chemistry approach, where the FGM [1] is the most widespread, and the ATFM [2]. The FGM is known for its computational efficiency related to the decoupling of the reaction time scale from the convection/diffusion ones, allowing the pre-tabulation of the chemistry. Despite that, important physical aspects having an impact on the flame brush (like stretch and heat loss) are not directly embedded into commercial codes and have to be introduced as customization [3]. On the other hand, the ATFM can naturally consider all these aspects and, more importantly, take care of preferential diffusion aspects, crucial for hydrogen combustion. The limitation of the latter model lies in its correct application only to perfectly premixed mixtures even if, recently, some dedicated variants have been proposed to overcome this issue [4]. From the computational cost perspective, surely the TFM implies higher costs, especially when detailed or skeletal mechanisms are considered.

In this work, detailed experimental measures related to an industrial burner are leveraged to compare the results provided by an enhanced version of both the FGM

and the ATFM. The mathematical formulation of the two approaches will be presented in the next paragraph which will be followed by a brief summary of the investigated test conditions. The Results and Discussion section will provide a detailed comparison among the models in terms of flame morphology, thermal, mixing, and velocity fields.

Test Rig Conditions

Tests are performed in an optically accessible rig with an industrial burner fed through two fuel lines [5]. The main pre-mixer injects the fuel through the counter-rotating swirler to deliver a uniform mixture into the combustor. Conversely, the pilot line is responsible for the flame stabilization delivering the gas directly into the primary zone. Figure 1 sketches the assembly of the main components of the dome as well as the computational grid in a longitudinal plane where the different sizing in the different regions of the model can be appreciated. The mesh is the same for all the investigated combustion models.

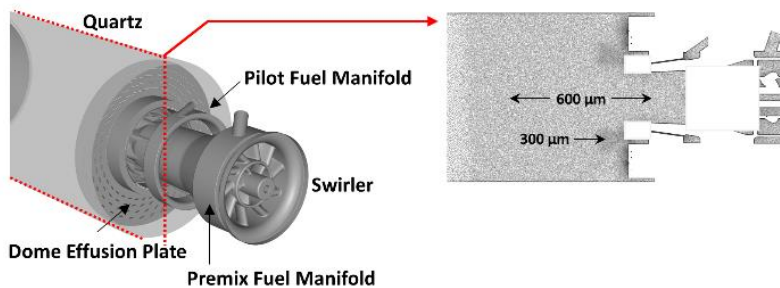


Figure 1. Detailed view of the burner-dome assembly and view of the grid in a longitudinal plane.

The rig is operated at atmospheric pressure, with the air temperature set to 300 °C and pure methane as fuel. A Horiba is used to analyze the flue gas, sampled after about 9 ms of residence time, and to retrieve the main pollutant emissions like CO and NO_x. The chemiluminescence is executed through a Phantom MIRO M340 camera and an intensifier equipped with a filter at 310 nm. Images are collected at 1000 Hz, with the gain and the gate set to 5 and 0.5 ms, respectively.

Mathematical Formulations of the Tested Combustion Models

Extended-ATFM

The approach presented in [4] is applied in the present study. A flame index is employed to identify the cell-based combustion regime: for positive values, the original formulation is applied [2] with the flame thickness discretized through 9 mesh points. Instead, the flame front is not thickened (consequently a finite-rate closure is adopted) when the diffusive regime is detected. A 19 species – 62 reactions skeletal mechanism derived ad-hoc for this investigation is used for the methane-air oxidation.

Extended-FGM-FR

This study exploits an enhanced version of the conventional FGM approach that incorporates the effects of flame stretch and heat loss in a pre-calculated table (Γ -table), thus directly impacting the combustion process reactivity. For this purpose, a new parameter (Γ) is defined and tabulated as a function of the strain rate k and heat loss ψ in order to correct the turbulent progress variable source term:

$$\widetilde{\omega}_c(\tilde{Z}, \tilde{c}) = \Gamma(\psi, k) \iint \widetilde{\omega}_c(Z, c) P(Z) P(c) dZ dc \quad (1)$$

with $\Gamma(\psi, k)$ multiplying the standard Finite Rate (FR) turbulent source term extracted from the look-up table. $\Gamma(\psi, k)$ is defined as the ratio between the maximum values of the strained, non-adiabatic progress variable source term and the adiabatic, unstrained one in a 1D laminar flame:

$$\Gamma(\psi, k) = \frac{\max \omega_c(Z, c, \psi, k)}{\max \omega_c^0(Z, c)} \quad (2)$$

with ψ identifying the heat loss parameter, defined as the ratio between the burnt gas temperature and the corresponding equilibrium value, and k representing the strain, evaluated from the velocity flow field according to [6]. Cantera libraries are used to solve several freely propagating flames ($k = 0$) and premixed counterflow flames ($k > 0$) in order to generate the $\Gamma(\psi, k)$ table. More details are available in [7].

Results and Discussion

Flame Morphology and thermal field

The prediction of the flame shape and position of the two numerical models against the measurements is reported in Figure 2.

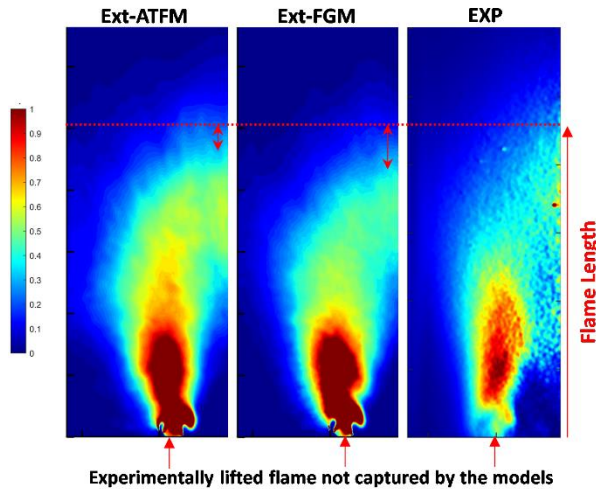


Figure 2. Normalized time-averaged heat release rate from the ATFM (left) and the Ext-FGM (center) compared with the Abel-deconvoluted OH* from the test (right).

The experimental map is the Abel-deconvoluted OH^* signal acquired with the camera placed orthogonally to the combustor axis. This map is compared with the time-averaged contour plots of the heat release on the midplane, shown in Fig. 1. To enable effective visual comparison between computed and experimental results, only half of the domain is reported. Both the combustion models predict the flame length reasonably well: the Ext-FGM has a higher underprediction of such quantity with respect to the ATFM, meaning that the former approach is affected by a higher reactivity. More importantly, despite both models can identify the main flame stabilization around the pilot jets, the experiments reveal that the corresponding heat release is more lifted. Numerically, the heat release reaches the peak value right downstream of the pilot fuel injection. Surely, such a finding is influenced by the adiabatic thermal boundary condition imposed on the burner wall of both models, adopted since no direct measure of the wall temperature is available in that position. The enhanced reactivity of the FGM has a direct impact on the thermal field. Figure 3 reports the contour plot of the time-average temperature in a longitudinal and in a cross-section inside the primary zone of the flame tube. Both these locations highlight that the peak temperature is higher for the FGM model compared with the ATFM all around the pilot-stabilized region. This behavior can potentially have an impact on the prediction of pollutant emissions, especially for NO_x .

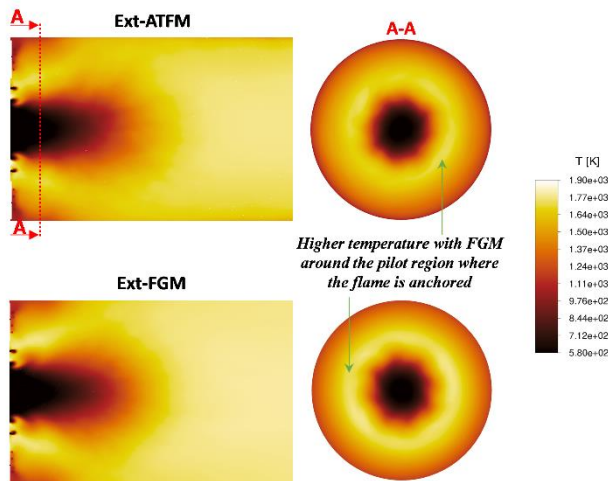


Figure 3. Time-averaged temperature field in a longitudinal and a transversal plane within the primary zone for both the numerical models.

Mixing and Velocity Field

The minor differences in the flame shape prediction between the two models do not appear to significantly affect the flow field in the burner exit region. Moreover, the flow fields within the combustion chamber exhibit strong agreement between the two numerical approaches, with only a few small discrepancies. Along the centerline ($Z = 0$), corresponding to the main region, the ATFM model exhibits a more axially

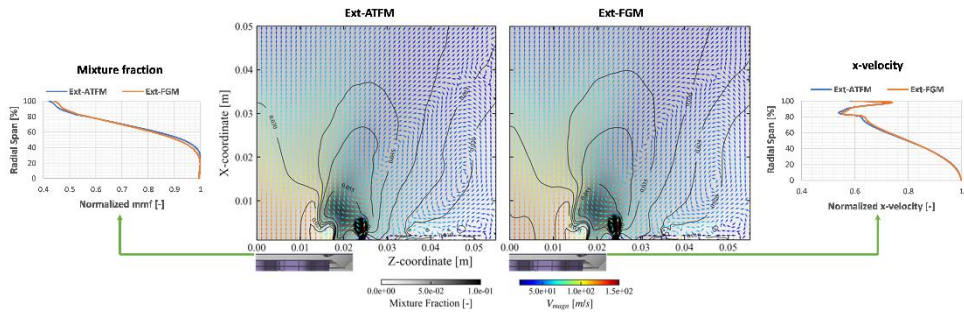


Figure 4. Time-averaged mixture fraction field and planar velocity vector-plot in a longitudinal plane within the primary zone for both the numerical models. Normalized mean values are plotted along the radius in a transversal section located at the main burner exit.

developed fluid region outside the main burner characterized by higher values of mixture fraction compared to the FGM model. Conversely, in the pilot region, the zone with higher mixture fraction values appears to be shorter for the ATFM model. These observations suggest that in the ATFM model, the pilot flame mainly enriches the main region rather than the recirculation zone.

Conclusion

In this work, an assessment of the flame shape prediction of two enhanced versions of the FGM and ATFM combustion models is performed through a direct comparison between the computed results and experimental data obtained from an in-house test rig.

Both models are capable of accurately predicting the flame topology, with ATFM showing slightly higher accordance with the experimental measurements compared to the FGM, the latter marginally underestimating the flame length, thus indicating a higher reactivity affecting the approach. The small discrepancies observed in predicting the flame shape between the two models do not seem to have a substantial impact on the flow field in the burner exit region.

It is important to note that the exclusion of wall heat losses from the analysis may impact the flame shape, and further investigations for both models will be carried out to estimate this effect.

Nevertheless, the FGM has shown its suitability for design-phase simulations by reasonably replicating the results from more computationally intensive models, such as the ATFM.

Nomenclature

ATFM Artificially Thickened Flame Model
CFD Computational Fluid Dynamics
FGM Flamelet Generated Manifold

<i>FR</i>	Finite Rate
<i>LES</i>	Large Eddy Simulation
<i>P</i>	Probability Density Function
<i>Z</i>	Mixture Fraction
ω	Source Term

Subscripts

<i>c</i>	Progress variable
----------	-------------------

Superscripts

<i>o</i>	Adiabatic unstrained
\sim	Mean value

References

- [1] J. A. V. Oijen and L. P. H. D. Goey, "Modelling of Premixed Laminar Flames using Flamelet-Generated Manifolds," *Combustion Science and Technology*, vol. 161, no. 1, pp. 113-137, 2000
- [2] O. Colin, F. Ducros, D. Veynante and T. Poinso, "A thickened flame model for large eddy simulations of turbulent premixed combustion," *Physics of Fluids*, vol. 12, no. 7, pp. 1843-1863, 2000
- [3] N. Klarmann, B. T. Zoller and T. Sattelmayer, "Numerical modeling of CO-emissions for gas turbine combustors operating at part-load conditions," *Journal of the Global Power and Propulsion Society*, vol. 2, pp. 376-387, 2018
- [4] A. Aniello, D. Laera, S. Marragou, H. Magnes, L. Selle, T. Schuller and T. Poinso, "Experimental and numerical investigation of two flame stabilization regimes observed in a dual swirl H₂-air coaxial injector," *Combustion and Flame*, vol. 249, 2023
- [5] S. Romano, R. Meloni, G. Riccio, P. C. Nassini and A. Andreini, "Modeling of Natural Gas Composition Effect on Low NO_x Burners Operation in Heavy Duty Gas Turbine," *Journal of Engineering for Gas Turbines and Power*, vol. 143, no. 3, 2021
- [6] P. C. Nassini, D. Pampaloni, R. Meloni and A. Andreini, "Lean blow-out prediction in an industrial gas turbine combustor through a LES-based CFD analysis," *Combustion and Flame*, vol. 229, no. 111391, 2021.
- [7] M. Amerighi, P. C. Nassini, A. Andreini, S. Orsino, I. Verma, R. Yadav and S. Patil, "Assessment of Flamelet Generated Manifold approach with inclusion of stretch effects of pure hydrogen flames," in *ASME Turbo Expo 2023 Turbomachinery Technical Conference and Exposition (GT2023)*, Boston, MA, 2023